ELSEVIER

Journal of Hydrology 259 (2002) 49–65

Journal of Hydrology

www.elsevier.com/locate/jhydrol

Flow of variable-density formation water in deep sloping aquifers: minimizing the error in representation and analysis when using hydraulic-head distributions

Stefan Bachu*, Karsten Michael

Alberta Energy and Utilities Board, Alberta Geological Survey, 4th Floor, Twin Atria, 4999-98 Avenue, Edmonton, Alta., Canada T6B 2X3

Received 9 January 2001; revised 2 September 2001; accepted 12 November 2001

Abstract

Although not fully adequate, freshwater hydraulic heads have been used historically to represent and analyze variable-density flow in sloping aquifers in sedimentary basins. The use of environmental heads is valid only for strictly vertical flow in unconfined aquifers, while using variable-density hydraulic heads contravenes Darcy's law. Although the use of hydraulic-head surfaces is the simplest and quickest means of flow analysis and interpretation, preceding other methods such as numerical modeling, it introduces some errors that should be assessed and minimized in order to provide the most accurate flow representation. A first error is introduced when approximating the potential and buoyancy components along aquifer slope of the flow-driving force with their projections onto the horizontal plane. This error is most probably negligibly small for sloping aquifers in undisturbed sedimentary basins, but may be significant for aquifers dipping at a significant angle, such as in folded strata. A second error is introduced when using only hydraulic heads in the representation and analysis, and neglecting the buoyancy component of the flow-driving force. The significance of this error can be assessed by performing a Driving Force Ratio (DFR) analysis. There is no single or critical value of the DFR, below which the error in using hydraulic heads alone is negligible, and above which it is not acceptable anymore; rather, the decision regarding the error acceptability should and can be made on a case by case basis. The DFR, hence the errors in flow direction and magnitude, can be minimized for any given aquifer by using an optimum reference density in hydraulic-head calculations that is the areally-weighted average density of formation water in that aquifer. In flow analyses based on potentiometric surfaces, the use of freshwater as the reference density actually maximizes the errors introduced by the neglect of the buoyancy component of the flow-driving force because it is either at the low end of the density-variation spectrum or outside it.

Keywords: Variable-density flow; Sloping aquifers; Hydraulic heads; Reference density

1. Introduction

Formation water in deep, regional-scale aquifers in sedimentary basins has usually a gradually-variable density as a result of areal variability in geothermal gradients, increase in temperature with depth, and variations in water salinity that can reach values >300,000 mg/l in the vicinity of salt beds and domes. The worldwide variation range of formation water density in sedimentary basins is from less than 940 kg/m^3 at >5000 m depth in a basin flushed by meteoric water, such as the Llanos in Colombia, to >1300 kg/m^3 in aquifers adjacent to salt beds like the

* Corresponding author. Fax: +1-780-422-1459.
E-mail address: stefan.bachu@gov.ab.ca (S. Bachu).

0022-1694/02/$ - see front matter
PII: S0022-1694(01)00585-6

Alberta and Williston basins (Bachu, 1995a,b; Bachu and Hitchon, 1996). The buoyancy effect of these density variations affects the magnitude and direction of the flow of formation water induced by other flow-driving mechanisms (e.g. Lahm et al., 1998). Buoyancy always acts in the direction of maximum aquifer slope, either downdip or updip, depending on the distribution of formation water density. Although the effect of density differences can sometimes be significant, many hydrogeological studies neglect to account for them and address the groundwater flow in deep sloping aquifers by considering the water as having constant density. With this assumption, a flow field potential can be defined and described mathematically, leading to the widespread use of equivalent hydraulic-head surfaces to represent and analyze the flow on the basis of freshwater hydraulic heads calculated using a standard density $\rho_f = 1000\ kg/m^3$.

The use of hydraulic heads for the analysis of formation-water flow is acceptable for horizontal and near-horizontal aquifers because hydraulic heads still provide a proper representation of the lateral flow (Lusczynski, 1961; DeWiest, 1965). The errors introduced by the use of equivalent hydraulic-head surfaces increase for sloping aquifers and for significant density differences (Jorgensen et al., 1982; Davies, 1987; Oberlander, 1989). Recognizing that buoyancy cannot be neglected in such cases, the flow of variable-density formation water was analyzed in most cases in the last two decades using numerical models rather than equivalent hydraulic-head surfaces. The most general approach is to revert to primary variables, such as pressure, temperature and concentration (e.g. Garven and Freeze, 1984; Bethke, 1985; Deming and Nunn, 1991; Lahm et al., 1998). This approach is computationally the most intensive because two or three partial differential equations have to be solved in two- or three-dimensional systems. In a different approach, Frind and Matanga (1985) and Senger and Fogg (1990a,b) developed a numerical model based on stream functions, rather than hydraulic heads, and relative density to find flow velocities in a steady-state flow system along a cross-section through a sedimentary basin. This way the problem of establishing the flow path on the basis of hydraulic-head distributions is circumvented by calculating directly the stream functions. Kuiper (1983) developed a three-dimensional model to simulate the flow of variable-density water in sloping aquifers by decomposing the flow rate as defined by Darcy's law into a vertical component and two orthogonal components in the bedding plane at small angles with the horizontal. The variables in Kuiper's model are pressure head and the ratio of water density to that of freshwater. Kuiper's model was used to simulate variable-density flow in US midcontinent basins (Gupta and Bair, 1997). Although Senger and Fogg, (1990a,b) and Kuiper's (1983) approaches solve only one partial differential equation in two and three dimensions, respectively, they are still computationally intensive. Moreover, all numerically-based methods require knowledge of the pressure (or hydraulic head) and density (or temperature and/or salinity) fields at every grid-point in the system, and of permeability or hydraulic conductivity.

The flow analysis based on numerical modeling is an extremely valuable tool for the analysis of theoretical cases that cannot be solved analytically and for the advance of general knowledge. However, in some cases they are difficult to apply because of a combination of system complexity, medium heterogeneity, general lack of data (particularly rock properties) and uneven data distribution. This is mostly the case of sedimentary basins, which are very large by comparison to usual shallow groundwater situations, and where the data are collected mainly by the energy industry for a different purpose. In these cases the flow representation and analysis is still based on potentiometric surfaces constructed on the basis of hydraulic-head distributions. Bachu (1995a) has shown that freshwater hydraulic heads correctly represent the horizontal components of variable-density flow in sloping aquifers, while environmental hydraulic heads correctly describe the vertical component (environmental hydraulic heads are calculated using a depth-averaged density as reference; Lusczynski, 1961). However, both fail to describe the flow in the other plane (vertical for freshwater hydraulic heads, and horizontal for environmental heads) and, consequently, the lateral flow along bedding in a sloping aquifer. In addition, the use of environmental hydraulic heads, besides being cumbersome, is inappropriate for the case of deep aquifers that are not in direct hydraulic communication with the ground surface (Bachu, 1995a). Hydraulic-head distributions remain

the only tool available for the representation and analysis of variable-density flow in sloping aquifers (Bachu, 1995a), provided that a dimensionless driving-force ratio (DFR) does not exceed a threshold value found numerically by Davies (1987) to be around 0.5. The DFR is an expression of the interplay between buoyancy, aquifer geometry and hydraulic gradients.

This paper examines the appropriateness of and methods for minimizing the errors introduced by using potentiometric surfaces based on hydraulic-head distributions in the representation and analysis of variable-density flow in sloping aquifers. The subscripts 'o' and 'f' are used in the following with respect to (any) reference and freshwater (1000 kg/m^3) densities, and the subscripts 'p' and 'b' are used to denote 'potential' and 'buoyancy', respectively.

2. Variable-density flow in sloping aquifers

The flow of fluids in porous media is described by the empirical Darcy's law in its most general form (Bear, 1972; de Marsily, 1986; Bachu, 1995a) that links the flow with its conjugated and non-conjugated forces. A flow potential or a force potential driving the flow of a variable-density fluid can be defined only for horizontal, stratified flow in a vertically stratified (layered) medium (Bachu, 1995a), in which case the flow can be described by a potentiometric surface. This extremely particular case is not found in sedimentary basins, and more so in sloping aquifers.

If a hydraulic head H_o is defined at every point with respect to a reference density ρ_o by:

$$H_o = \frac{p}{\rho_o g} + z \tag{1}$$

where p is pressure, z is elevation and g is the gravitational constant, then, neglecting osmotic flow (Bear, 1972; de Marsily, 1986; Neuzil, 1986), Darcy's law is reduced to its well known form, expressed in terms of hydraulic head:

$$\mathbf{q} = -\frac{k\rho_o g}{\mu}\left(\nabla H_o + \frac{\Delta\rho}{\rho_o}\nabla z\right) \tag{2}$$

In the previous equation k is rock permeability, μ is water viscosity, $\Delta\rho = \rho - \rho_o$ is the difference between the actual water density ρ and the reference density ρ_o, and z this time is the vertical coordinate directed upwards (de Marsily, 1986, p. 56). The force driving the flow, per unit mass, is given (Hubbert, 1940, 1953, 1956) by:

$$\mathbf{F} = -\frac{g\rho_o}{\rho}\left(\nabla H_o + \frac{\Delta\rho}{\rho_o}\nabla z\right) \tag{3}$$

For aquifers of large areal extent compared with their vertical dimension, as is the case in sedimentary basins, the aquifer thickness and density variations along the vertical are generally negligible and the flow can be considered as two-dimensional in the bedding plane. The driving force $\mathbf{F}$ and the specific discharge $\mathbf{q}$ can be decomposed into components in the bedding rather than the horizontal plane (Kuiper, 1983; Dorgarten and Tsang, 1991). Because these components are difficult to evaluate, and owing to the small angles of sloping aquifers in sedimentary basins, they can be approximated by using their gradients in the horizontal plane (Bachu, 1995a), such that the previous relation can be written directly in vectorial form as:

$$\mathbf{F} = -\frac{g\rho_o}{\rho}\left(\nabla H_o + \frac{\Delta\rho}{\rho_o}\nabla E\right) \equiv \mathbf{F}_p + \mathbf{F}_b \tag{4}$$

where $E(x, y)$ is the surface describing the sloping aquifer, and the gradient is taken in the horizontal plane only. The corresponding form of Darcy's law for variable-density flow along bedding in sloping aquifers is:

$$\mathbf{q} = \frac{k\rho}{\mu}\mathbf{F} \equiv -\frac{k\rho_o g}{\mu}\left(\nabla H_o + \frac{\Delta\rho}{\rho_o}\nabla E\right) \tag{5}$$

The earlier expressions show that the flow of formation waters in sedimentary basins is driven along aquifer bedding by a potential force $\mathbf{F}_p$ caused by pressure and/or position (topographic) differences, and by a buoyancy force $\mathbf{F}_b$ caused by density differences. The potential force drives flow in the direction of maximum hydraulic gradient, while buoyancy drives flow in the direction of maximum aquifer slope. The DFR is the ratio of buoyancy to potential forces, defined as (Davies, 1987; Bachu, 1995a):

$$\mathrm{DFR} = \frac{\Delta\rho}{\rho_o}\frac{|\nabla E|}{|\nabla H_o|} \tag{6}$$

The DFR was used by Davies (1987) as an indicator of

error significance in neglecting buoyancy and using only freshwater hydraulic-head surfaces when representing and analyzing variable-density flow in sloping aquifers. In this case Darcy's law reverts to:

$$\mathbf{q} = -\frac{k\rho_o g}{\mu}\nabla H_o \equiv \frac{k\rho}{\mu}\mathbf{F}_p \tag{7}$$

On the basis of numerical experiments for the Yucca Mountain nuclear repository, Davies (1987) concluded that $DFR_{cr} = 0.5$ is a threshold, or critical value, above which the errors would become significant and buoyancy cannot be neglected any longer. However, Davies (1987) recognized that this threshold value is arbitrary and that for each case a different DFR_{cr} value can be chosen, depending on the problem at hand. The DFR is relatively easy to calculate based on water density distribution, freshwater hydraulic-head surface and aquifer structure top (or bottom). As it will be seen later, the DFR provides a measure of error significance, and in certain particular cases it represents the maximum possible error in force magnitude or deviation, whereas the actual errors can be smaller depending on the orientation between the components of the flow-driving force.

3. Reference density and associated errors

A generalization of Jorgensen et al. (1982) simple case of two wells sampling an aquifer containing water of constant density $\rho_c > \rho_f$ provides an illustrative example which shows that the use of freshwater hydraulic heads introduces errors in the study of flow in sloping aquifers whose water density is different from ρ_f. In a hydrostatic system ($\mathbf{q} \equiv 0$) where:

$$\mathbf{q} = -\frac{k\rho_f g}{\mu}\left(\nabla H_f + \frac{\rho_c - \rho_f}{\rho_f}\nabla E\right) \equiv 0 \tag{8}$$

hence

$$\nabla H_f = -\frac{\Delta\rho}{\rho_f}\nabla E \neq 0 \tag{9}$$

the gradient of freshwater hydraulic heads, ∇H_f, is different from zero. Thus, the freshwater hydraulic-head surface will indicate updip flow when in reality none exists. On the other hand, choosing the actual density ρ_c as the reference density ρ_o will correctly show no flow since $\Delta\rho = 0$ and $\nabla H_c = 0$. This result can be easily extended to a static system in a sloping aquifer containing variable-density water. This simple example shows that the use of freshwater density as a reference density ($\rho_o = \rho_f$) introduces an artificial buoyancy-term into the system, which distorts the potential force and, consequently, the resulting flow field if it is described only by the hydraulic-head surface.

Recognizing that freshwater hydraulic heads, H_f, do not incorporate spatial variations in fluid density, Gupta and Bair (1997) used variable-density heads, H_v, to study the flow of formation water in the Mt. Simon Sandstone Formation in the US midcontinent. The variable-density heads were calculated using in relation (1) the actual water density ρ at each measurement point, instead of a constant reference density across the entire flow field. Flow directions inferred from this 'potentiometric' surface indicated flow downdip into the midcontinent basins, while the potentiometric surface based on freshwater hydraulic heads showed updip flow, out of the Illinois, Michigan and Appalachian basins (Gupta and Bair, 1997). Subsequent numerical simulations based on Kuiper's (1983) model led Gupta and Bair (1997) to conclude that the variable-density "potentiometric map alone is not sufficient to determine reliable flow patterns" and that "a more accurate determination of the magnitude and direction of flow is obtained by plotting Darcy velocity vectors calculated from the simulated variable-density fluxes".

The paradoxical results obtained by Gupta and Bair (1997) are easy to explain if one considers the following.

1. Since neither a flow potential nor a force potential exist for variable-density flow (Bachu, 1995a), by definition the surface constructed on the basis of variable-density hydraulic heads H_v is not a potentiometric surface, although labeled as such; hence flow directions cannot be inferred on the basis of that surface's gradients.
2. The very use of variable-density hydraulic heads H_v in the flow analysis is wrong because it contravenes Darcy's law for flow in porous media by introducing an additional artificial term. If, in Darcy's law, the variable-density hydraulic head H_v is substituted instead of a constant-density hydraulic-head H_o, an additional term is obtained

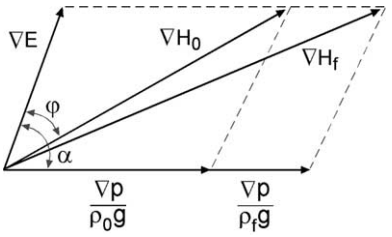

Fig. 1. Dependence of the hydraulic-head gradient, ∇H_o, in position and magnitude, on the choice of the reference density ρ_o.

beside the specific discharge **q**:

$$-\frac{k\rho g}{\mu}\nabla H_v = -\frac{k\rho g}{\mu}\left(\frac{\nabla p}{\rho g} - \frac{p\nabla\rho}{\rho^2 g} + \nabla z\right) \equiv \mathbf{q} + \frac{kp\nabla\rho}{\mu\rho} \quad (10)$$

Thus, it is evident that only a constant reference-density value ρ_o can be used in the construction of distributions of hydraulic heads to describe, albeit with approximations, variable-density flow.

Having established on the basis of the above that a constant reference density has to be used in the representation and analysis of variable-density flow in sloping aquifers, two issues should be addressed:

1. how large is the error introduced by using a constant reference density; and
2. what is the reference value ρ_o that will minimize the errors.

Answering these questions will indicate whether or not the freshwater density ρ_f is the best choice for the reference value to be used in the analysis of variable-density flow based on hydraulic heads alone. Examples from Jorgensen et al. (1982), Oberlander (1989), Senger and Fogg (1990a,b), and Ophori (1999) already intuitively suggest that it is not.

Because freshwater ($\rho_f = 1000\ \mathrm{kg/m^3}$) has been used in the past as the reference state for water, the following variables will be used further in the analysis, to allow mathematical manipulation and generalization of results:

(a) freshwater pressure head, $h_f = p/\rho_f g$, which is the pressure component of the freshwater hydraulic head;
(b) dimensionless density: $\rho^* = \rho/\rho_f$, hence $\rho_o^* = \rho_o/\rho_f$;
(c) ratio of aquifer slope to the gradient of freshwater pressure head, $\mathrm{RSH} = |\nabla E|/|\nabla h_f|$;
(d) magnitude M_{Ho} of the hydraulic gradient compared with the gradient of the freshwater pressure head: $M_H = |\nabla H|/|\nabla h_f|$, hence $M_{Ho} = |\nabla H_o|/|\nabla h_f|$.
(e) DFR relation (6);
(f) magnitude M_E of buoyancy along slope at any reference density compared to the buoyancy at freshwater density: $M_E = [(\rho - \rho_o)|\nabla E|/\rho_o]/[(\rho - \rho_f)|\nabla E|/\rho_f] = (\rho^*/\rho_o^* - 1)/(\rho^* - 1)$.

3.1. Dependence of the potential and buoyancy components of the flow-driving force on the reference density

The driving force **F** can be decomposed into potential and buoyancy components, $\mathbf{F}_p$ and $\mathbf{F}_b$ (relation (4)), in the space of coordinates x, y and ρ_o. The values and directions of these components depend on the position and magnitude of the driving force **F** and on the value of the reference density ρ_o. Both the direction and magnitude of ∇H_o change with the choice of a different reference density because the shape of the hydraulic-head surface changes with the choice of a different reference density ρ_o. Since the aquifer elevation is described by the surface $z = E(x, y)$, the hydraulic gradient in the horizontal plane becomes:

$$\nabla H_o = \frac{\nabla p}{\rho_o g} + \nabla E \equiv \frac{\nabla h_f}{\rho_o^*} + \nabla E \quad (11)$$

This relation shows that, because both ∇E and ∇h_f are constant in magnitude and direction at any point described by its position (x, y), the magnitude of ∇H_o decreases and its direction shifts toward ∇E as ρ_o^* increases (Fig. 1). It also shows that the ratio of aquifer slope to the gradient of freshwater pressure head, RSH, is an indicator of the relative strength of the two components of the potential driving force, $\mathbf{F}_p$, the one resulting from position differences and the one resulting from pressure differences caused by other driving mechanisms (e.g. compaction).

If ∇h_f is at an angle α with ∇E, then the magnitude M_o of ∇H_o and the angle φ between ∇H_o and ∇E are

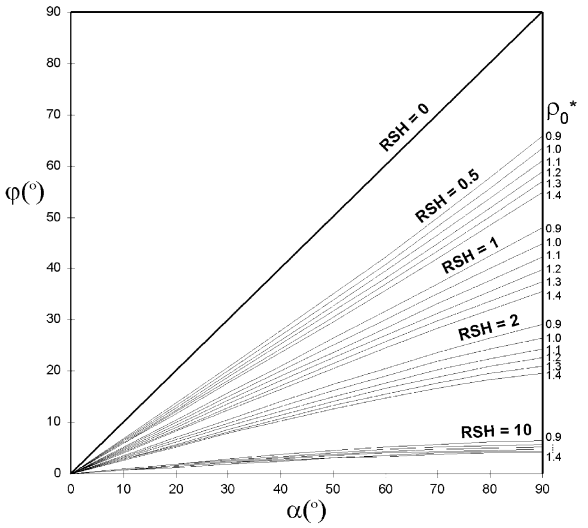

Fig. 2. Dependence of the angle φ between the hydraulic gradient, ∇H_o, and aquifer slope, ∇E, on: the angle α between the latter and the gradient of freshwater pressure head, ∇h_f, the ratio RSH of aquifer slope to the gradient of freshwater pressure head, and the reference density ρ_o^* (relation (12)).

given by:

$$\tan\varphi = \frac{\dfrac{|\nabla h_f|}{\rho_o^*}\sin\alpha}{\dfrac{|\nabla h_f|}{\rho_o^*}\cos\alpha + |\nabla E|} \equiv \frac{\sin\alpha}{\cos\alpha + \rho_o^* \mathrm{RSH}} \tag{12}$$

and

$$M_{Ho} \equiv \frac{|\nabla H_o|}{|\nabla h_f|} = \frac{\sin\alpha}{\rho_o^* \sin\varphi} \equiv \frac{\cos\alpha + \rho_o^* \mathrm{RSH}}{\rho_o^* \cos\varphi} \tag{13}$$

Figs. 2 and 3a show graphically the decrease of both φ and M_{Ho} with the increase in the reference density ρ_o^* for various ranges of α and RSH. The case of an horizontal aquifer, where the hydraulic-head gradient maintains its direction, and where its magnitude is proportional to the reference density, is easily retrieved from the earlier relations for RSH = 0 (i.e. $\varphi = \alpha$ and $M_o = 1/\rho_o^*$, see also Figs. 2 and 3a). Thus, for a range of reference-density values ($\rho_{min} < \rho_o < \rho_{max}$), ∇H_o at any point will have a maximum magnitude for $\rho_o = \rho_{min}$ and it will be at the largest angle with the aquifer slope. If $\rho_o = \rho_{max}$, then the magnitude of ∇H_o will be the lowest, and its direction will be the closest to ∇E.

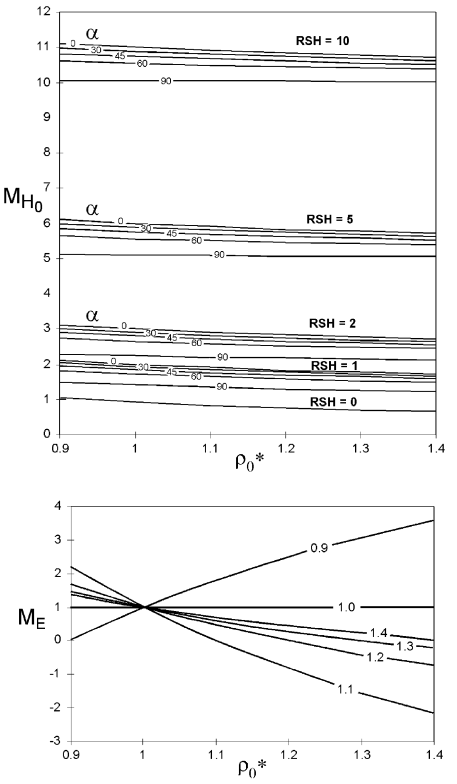

Fig. 3. Dependence on the reference density ρ_o^* of the relative magnitude of: (a) the hydraulic gradient, M_{Ho}; and (b) the buoyancy component, M_E, of the flow-driving force. Note that M_{Ho} depends also on the angle α between the aquifer slope, ∇E, and the gradient of freshwater pressure head, ∇h_f, and on the ratio RSH of aquifer slope to the gradient of freshwater pressure head (relation (13)). The direction of M_E also depends on the reference density (positive indicates updip, negative indicates downdip).

The direction of the buoyancy component $\mathbf{F}_b$ will always be along the aquifer slope ∇E. As long as $\rho_o < \rho$, the magnitude $(\rho - \rho_o)|\nabla E|/\rho_o$ of $\mathbf{F}_b$ will decrease as ρ_o increases. If at a particular point the reference density ρ_o happens to be equal to the actual density ρ, then $\mathbf{F}_b = 0$ and $\mathbf{F} = \mathbf{F}_p$ at that point. For $\rho_o > \rho$, the magnitude of $(\rho - \rho_o)|\nabla E|/\rho_o$ will start increasing again as ρ_o increases from ρ, albeit at a slower rate than the decrease for $\rho_o < \rho$. If $\rho > \rho_o$, then $\mathbf{F}_b$ will be oriented updip, otherwise it will be oriented downdip. Fig. 3b shows in dimensionless variables the variation in magnitude M_E and in direction (positive and negative values) of the buoyancy component of the driving force as a function of the reference density ρ_o, for various values of the local

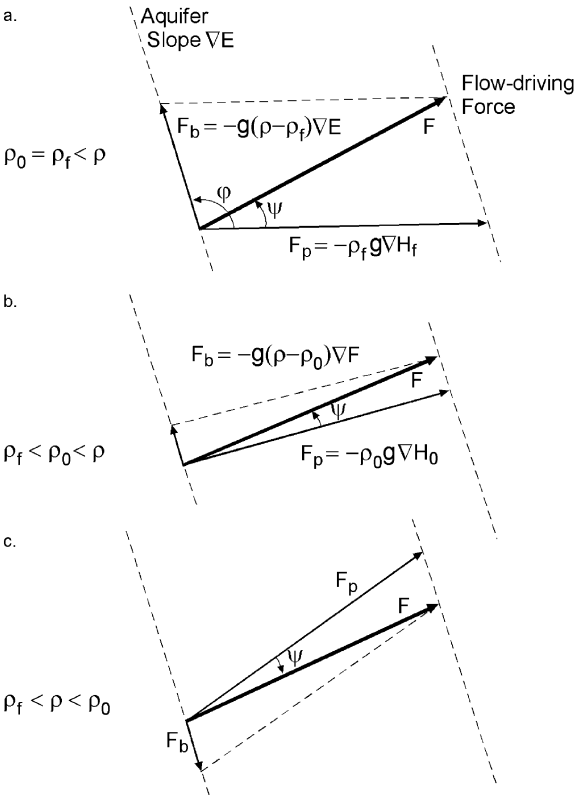

Fig. 4. Vector diagram showing the decomposition of the flow-driving force **F** into its potential and buoyancy components, $\mathbf{F}_p$ and $\mathbf{F}_b$, for various reference density values: (a) $\rho_o = \rho_f < \rho$; (b) $\rho_f < \rho_o < \rho$; and (c) $\rho_f < \rho < \rho_o$.

density ρ. Because of the choice of ρ_f as a reference density, the case of $\rho^* < 1$ appears in Fig. 3b as the mirror image, oriented updip, of the real situation when it is always oriented downdip.

The vector diagram of Fig. 4 shows that, theoretically, any value can be chosen for the reference density ρ_o, resulting in an infinite number of combinations into which the driving force **F** can be decomposed into potential and buoyancy components $\mathbf{F}_p$ and $\mathbf{F}_b$. If $\rho > \rho_o$, then $\mathbf{F}_b$ is oriented updip (Fig. 4a and b), otherwise it is oriented downdip (Fig. 4c), with a corresponding positioning of $\mathbf{F}_p$ at a positive or negative angle Ψ with **F**. This shows again that the potential and buoyancy terms in the driving force and in Darcy's law (relations (4) and (5)) are not independent, but are components of **F** and **q** with respect to a selected reference density.

3.2. Errors introduced by using hydraulic heads only in the study of variable-density flow in sloping aquifers

As mentioned previously, the DFR (relation (6)) is only a measure of the maximum possible error introduced by the use of hydraulic-head surfaces alone and neglect of the buoyancy component in the study of variable-density flow in sloping aquifers. Although it is already a dimensionless parameter, it can be expressed as a function of the previously-defined dimensionless variables and parameters as:

$$\mathrm{DFR} = \left(\frac{\rho^*}{\rho_o^*} - 1\right)\frac{\mathrm{RSH}}{M_{\mathrm{Ho}}} \tag{14}$$

In a horizontal system of coordinates with the x-axis along $\mathbf{F}_p$ (since ∇H_o is usually used in analysis), where $\mathbf{F}_b$ oriented along ∇E is at an angle φ with $\mathbf{F}_p$ (Fig. 5), the errors in direction (angle Ψ) and magnitude $|\mathbf{F}|/|\mathbf{F}_p|$ of the driving force, hence Darcy velocity, are

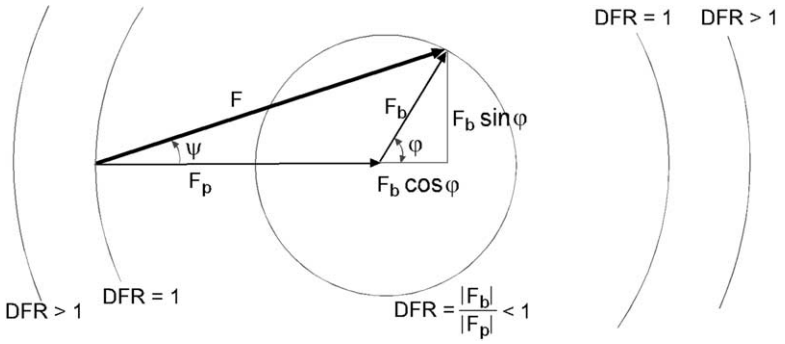

Fig. 5. Vector diagram showing the locus of all flow-driving forces **F** that decompose into buoyancy and potential components, $\mathbf{F}_p$ and $\mathbf{F}_b$, that have the same DFR.

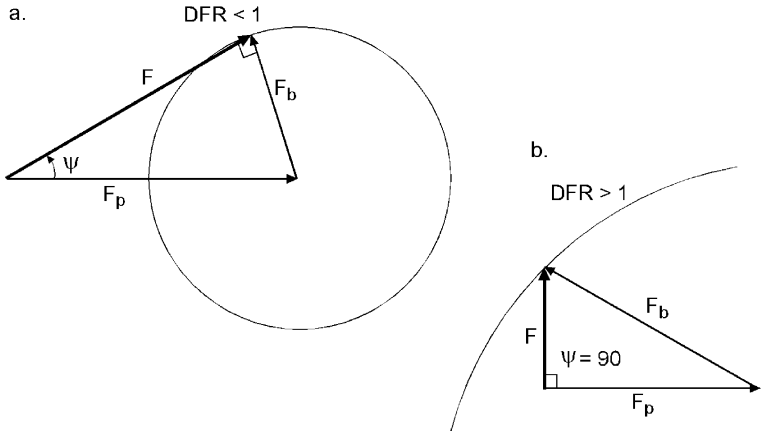

Fig. 6. Vector diagrams showing particular cases of relations between the driving force **F** and its potential and buoyancy components, $\mathbf{F}_p$ and $\mathbf{F}_b$: (a) when DFR < 1 and **F** is at a right angle with $\mathbf{F}_b$; and (b) when DFR > 1 and **F** is at a right angle with $\mathbf{F}_p$.

given by:

$$\tan \Psi = \frac{|\mathbf{F}_b| \sin \varphi}{|\mathbf{F}_p| + |\mathbf{F}_b| \cos\varphi} \equiv \frac{\text{DFR} \sin \varphi}{1 + \text{DFR} \cos \varphi} \qquad (15)$$

and

$$|\mathbf{F}| \cos \Psi = |\mathbf{F}_p| + |\mathbf{F}_b| \cos \varphi, \text{ or } |\mathbf{F}|$$
$$= |\mathbf{F}_h| \cos \Psi + |\mathbf{F}_b| \cos(\varphi - \Psi);$$

hence:

$$\frac{|\mathbf{F}|}{|\mathbf{F}_p|} = \frac{1 + \text{DFR} \cos \varphi}{\cos \Psi} \equiv \cos \Psi + \text{DFR} \cos(\varphi - \Psi) \qquad (16)$$

The earlier relations are valid for all possible relations and positions between $\mathbf{F}_p$ and $\mathbf{F}_b$, i.e. for any DFR value (both less and greater than unity) and angle φ between ∇H_o and ∇E ($0 < \varphi < 360$), except for the following cases of singularities in these expressions:

(a) when the driving force **F** is at 90° with its buoyancy component $\mathbf{F}_b$ for DFR < 1, i.e. for $\varphi - \Psi = 90°$ or 270°, when Ψ reaches its maximum value (Fig. 6a) and:

$$\sin \Psi_{max} = \pm \text{DFR} \qquad (17)$$

and

(b) when the driving force **F** is at 90° with its

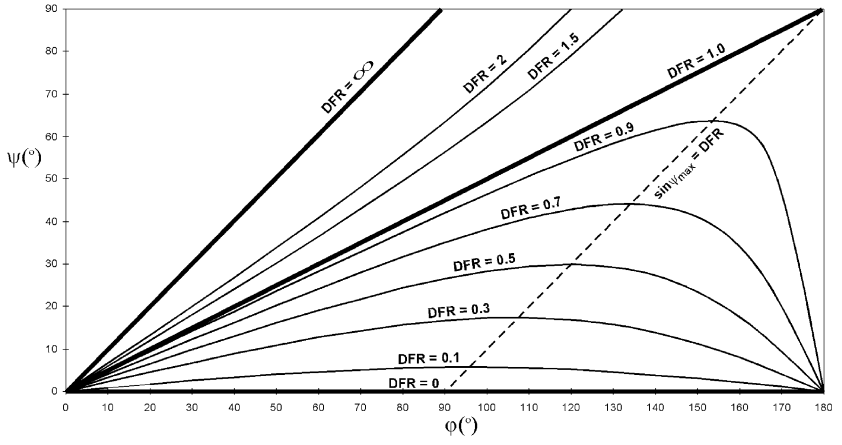

Fig. 7. Dependence of the error in the direction Ψ of the flow-driving force **F** on the angle φ between its potential and buoyancy components, $\mathbf{F}_p$ and $\mathbf{F}_b$, and on the magnitude of the DFR.

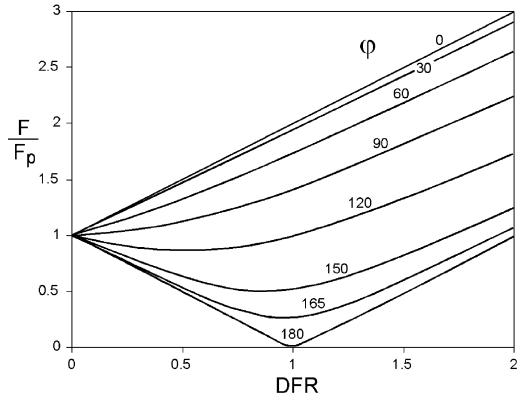

Fig. 8. Dependence of the error ϵ in magnitude of the flow-driving force $\mathbf{F}$ on the angle φ between its potential and buoyancy components, $\mathbf{F}_p$ and $\mathbf{F}_b$, and on the magnitude of the DFR.

potential component $\mathbf{F}_p$ for DFR > 1 (Fig. 6b), i.e. $\Psi = 90°$ or $\Psi = 270°(\cos\Psi = 0)$, when:

$$\frac{|\mathbf{F}|}{|\mathbf{F}_p|} = -\tan\varphi \tag{18}$$

The particular cases when the hydraulic gradient ∇H_o is along dip (colinear with ∇E) are easily retrieved from the general relations (15) and (16), leading to $\Psi = 0$ or $\Psi = 180°$, and $|\mathbf{F}|/|\mathbf{F}_p| = 1 \pm$ DFR, depending on the combination between $\varphi = 0$ or $\varphi = 180°$, and DFR < 1 or DFR > 1. Figs. 7 and 8 show, respectively, the dependence of the errors in the direction Ψ and magnitude $|\mathbf{F}|/|\mathbf{F}_p|$ on the angle φ between the potential and buoyancy components of $\mathbf{F}$, and on the DFR magnitude when using only hydraulic heads in the representation and analysis of variable-density flow in sloping aquifers. The cases of collinear $\mathbf{F}_p$ and $\mathbf{F}_b$ in the same and opposite directions ($\Psi = 0$ and $\Psi = 180°$, respectively) are clearly represented in Fig. 8 by the linear dependence of $|\mathbf{F}|/|\mathbf{F}_p|$ on DFR. As indicated earlier, $|\mathbf{F}|/|\mathbf{F}_p| = 1 \pm$ DFR and $\Psi =$ arcsin(DFR), represent, respectively, the maximum error in force magnitude and deviation that are introduced when neglecting the buoyancy term in the flow analysis.

3.3. Optimum reference water density

It is quite difficult to find the reference water density that will minimize the errors Ψ in flow direction and $\epsilon = |\mathbf{F}|/|\mathbf{F}_p| - 1$ in flow magnitude introduced by the use of hydraulic heads and neglect of the buoyancy component in the representation and analysis of variable-density flow in sloping aquifers. For an aquifer whose vertical dimension is negligible compared with its areal extent, the aquifer geometry $z = E(x, y)$ and distributions of water density $\rho = \rho(x, y)$ and of pressure $p = p(x, y)$, hence of freshwater pressure heads h_f, are the only known elements. On the basis of these distributions, the new 'independent' variables $\alpha = \alpha(x, y)$ and RSH $=$ RSH(x, y) can be calculated according to their definitions. Then, for a chosen reference density ρ_o, the following dependent variables can be successively calculated using relations (12)–(18):

$$\varphi = \varphi(\rho_o^*, \alpha, \text{RSH}) \equiv f_1(x, y, \rho_o^*)$$

$$M_{Ho} = M_{Ho}(\rho_o^*, \alpha, \text{RSH}) \equiv f_2(x, y, \rho_o^*)$$

$$\text{DFR} = \text{DFR}(\rho^*, \rho_o^*, \alpha, \text{RSH}) \equiv f_3(x, y, \rho_o^*)$$

$$\Psi = \Psi(\text{DFR}, \varphi) \equiv \Psi(\rho^*, \rho_o^*, \alpha, \text{RSH}) \equiv f_4(x, y, \rho_o^*)$$

$$\epsilon = \epsilon(\text{DFR}, \varphi, \Psi) \equiv \epsilon(\rho^*, \rho_o^*, \alpha, \text{RSH}) \equiv f_5(x, y, \rho_o^*)$$

Calculation of the errors Ψ and ϵ would be an intensive computational task akin to calculating the driving force $\mathbf{F}$ and Darcy velocity $\mathbf{q}$ everywhere in the aquifer, thus defeating the very purpose of using only the hydraulic-head surface in representing and analyzing the flow. Rather, the task is to find a priori the reference density $\rho_o = \rho_{opt}$ that minimizes the errors. For explicit and rather simple analytical functions, the value of the independent variable that minimizes that function can be found using standard mathematical methods based on differentiation. Unfortunately, the expressions of Ψ and ϵ are very complex and contain embedded transitive and inverse functions. In addition, the reference density that minimizes the error Ψ in flow direction is different from the reference density that minimizes the error ϵ in magnitude because Ψ and ϵ are not simultaneously at a minimum. For example, for DFR < 1 (Figs. 5 and 6a): when $\Psi = 0(\Psi_{min})$, then $|\epsilon| =$ DFR $\equiv \epsilon_{max}$; and when $\Psi = \Psi_{max}(\sin\Psi_{max} =$ DFR; relation (17)), then

$$|\epsilon| = |\cos\Psi_{max} - 1| < \sin\Psi_{max} = \text{DFR} \equiv \epsilon_{max}.$$

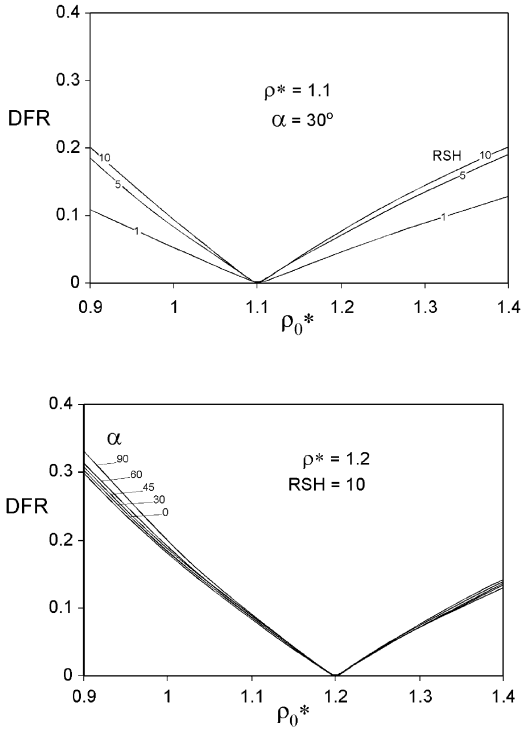

Fig. 9. Dependence of the local DFR at any location in an aquifer on local aquifer characteristics (slope, pressure-head gradient and water density) and choice of the reference density ρ_o^* : (a) for $\rho^* = 1.1$, $\alpha = 30°$ and various RSH values; and (b) for $\rho^* = 1.2$, RSH = 10 and various angles α between aquifer slope and the pressure-head gradient.

For these reasons, an optimum value $\rho_o = \rho_{opt}$ is sought that will provide the most accurate flow representation using hydraulic heads. Fortunately, relations (15)–(18), represented graphically in Figs. 7 and 8, show that the errors in both direction and magnitude of the flow-driving force **F**, hence of Darcy velocity **q**, that are introduced when hydraulic heads only are used in the representation and analysis of variable-density flow in sloping aquifers, increase, albeit differently, when the DFR increases. Thus, rather than directly seeking the value of the reference density ρ_o that minimizes both Ψ and ϵ, it is sufficient to find the value of ρ_o that minimizes the DFR.

Examination of relations (12)–(14) and of Figs. 2 and 3 shows that the DFR has a much stronger dependence on ρ_o^* than on α and RSH. Moreover, although the reference density ρ_o^* appears also in the denominator M_{Ho}, its effect manifests itself mainly through the difference $\Delta\rho$ between the local density ρ and the reference density ρ_o. Fig. 9 illustrates in dimensionless form the dependence of the DFR at any location in an aquifer, on the reference density and local density, aquifer slope and hydraulic-head gradient, as expressed by ρ_o^*, ρ^*, RSH and α. The quasi-linear dependence of DFR on the choice of reference density is due to the heavy weight of $\Delta\rho$ in relations (6) and (14) when compared with all other terms. Fig. 9 clearly shows that the closer the reference density value, ρ_o^*, is to the local density, ρ^*, (i.e. smaller $\Delta\rho$), the smaller is the local DFR. Thus, for a given aquifer, the optimum reference density, $\rho_o = \rho_{opt}$, that minimizes the DFR for the aquifer as a whole and renders the most accurate image of flow strength and direction when using hydraulic-head distributions is that reference density that minimizes the difference $\Delta\rho$ for the entire aquifer. This value, by definition, is the areally-weighted average value of the density-variation in the aquifer. Thus:

$$\min \int\int \mathrm{DFR}(\rho^*, \rho_o^*, \alpha, \mathrm{RSH})\mathrm{d}x\mathrm{d}y = \int\int \mathrm{DFR}(\rho - \rho_{opt})\mathrm{d}x\mathrm{d}y \tag{19}$$

where

$$\rho_{opt} = \frac{\int\int \rho \mathrm{d}x\mathrm{d}y}{\int\int \mathrm{d}x\mathrm{d}y} \tag{20}$$

This analysis shows that the use of freshwater hydraulic heads in the representation and analysis of variable-density flow in sloping aquifers actually maximizes the errors introduced by the neglect of the buoyancy component of the flow-driving force, thus distorting the flow field. This is not only because it represents an extreme rather than an average value, but also because usually it is outside the range of density-variation in such aquifers.

4. Example of application

This study of the appropriateness of using freshwater hydraulic heads in the representation and analysis of variable-density flow in sloping aquifers stemmed from the need to analyze the flow of formation waters in the Alberta basin which is located in

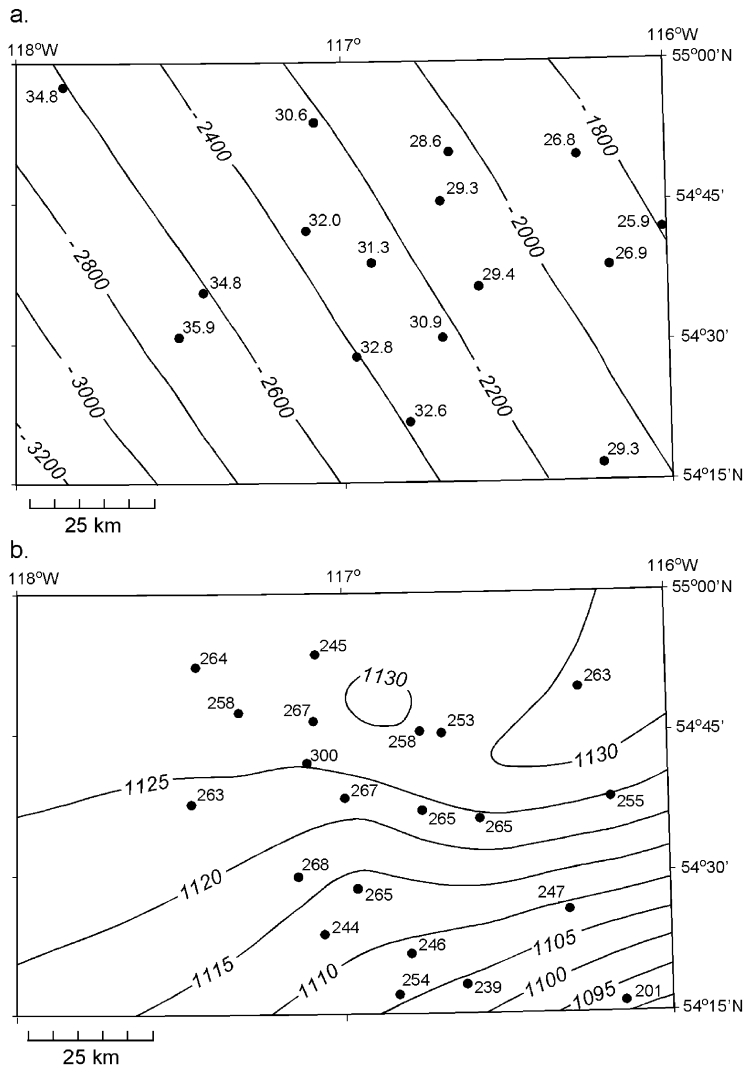

Fig. 10. Relevant characteristics of the Devonian Elk Point aquifer in the west-central part of the Alberta basin: (a) structure top contour lines (masl) and measured pressures (MPa); and (b) measured salinity (g/l) and contour lines of calculated density distribution (kg/m^3).

Canada east of the Rocky Mountains. The basin consists of a northeasterly tapering wedge of sedimentary rocks that reach >6000 m depth in the southwest near the Cordilleran thrust and fold belt. The salinity of formation waters varies from <1000 mg/l in shallow surface aquifers, to >350,000 mg/l in the vicinity of deep evaporitic beds, leading to corresponding water densities of up to ~1300 kg/m^3 (Bachu, 1995b). The flow of formation waters is extremely complex, being driven in local, intermediate and several basin-scale flow systems by topography, erosional rebound, past tectonic compression, and active hydrocarbon generation (Bachu, 1995b; Michael and Bachu, 2001). Because of the geological and hydrogeological complexity of the basin and of the flow systems, it is very difficult to use numerical modeling as a tool for representing and analyzing the flow. One has to rely on pressure and bottom hole temperature measurements, and analyses of formation waters from >200,000 wells drilled to date in the basin to analyze the flow and define the boundary and initial conditions necessary in any subsequent

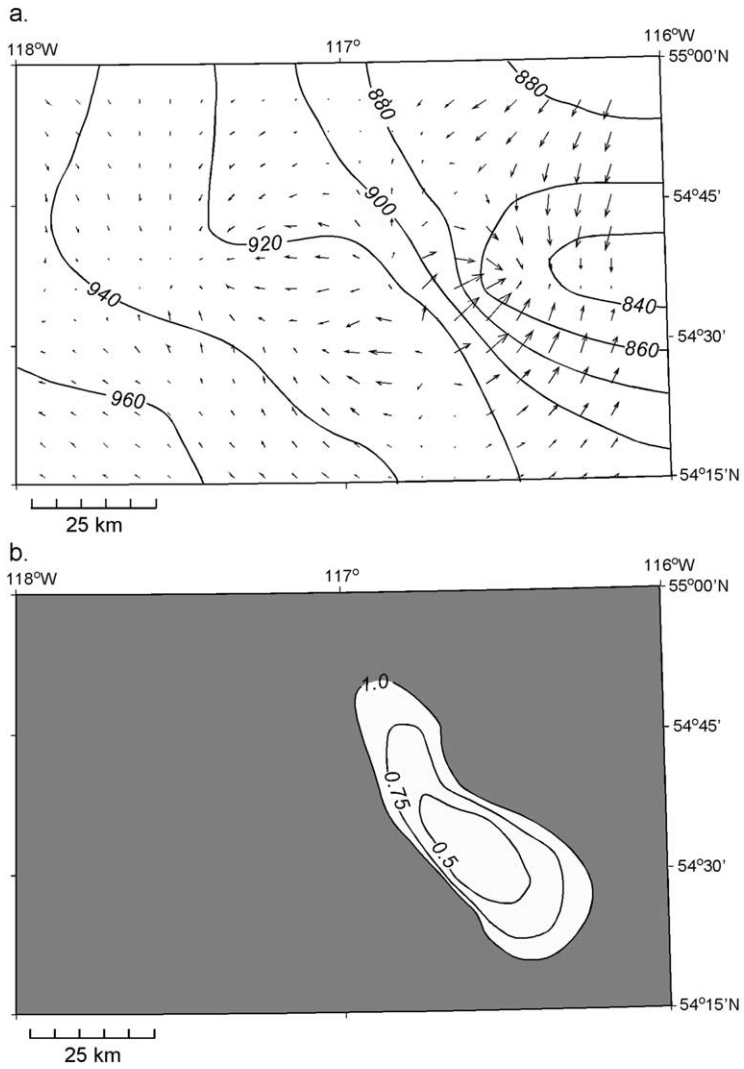

Fig. 11. Flow representation using the freshwater density, $\rho_f = 1000$ kg/m^3, as reference density: (a) distribution of hydraulic heads, overlain by the flow-driving force field; (b) distribution of the DFR. The shaded area represents DFR > 1.

modeling of basin evolution, hydrocarbon generation and migration, ore genesis, or fate of injected fluids.

The example chosen for illustration is for a part of the Devonian Elk Point aquifer found from ~2800 to ~3800 m depth in the west-central part of the basin, in an area of 80×130 km^2 defined by 116–118°W and 54°15′–55°N. The top structure of the aquifer varies between −3273 m in the SW and −1684 m in the NE, with an average slope of 10.9 m/km (Fig. 10a). Pressures measured in wells penetrating the aquifer vary between 25.9 and 35.9 MPa (Fig. 10a). The salinity of formation water measured in water samples varies from 201 to 300 g/l (Fig. 10b). The density of formation water, calculated (McCain, 1991) on the basis of pressure, salinity and temperatures derived from geothermal gradients (Bachu and Burwash, 1991), varies across the study area in the 1088–1136 kg/m^3 range, with an areal-average of 1121 kg/m^3 (Fig. 10b).

Distributions of hydraulic heads and DFRs were calculated for the following reference densities: (a) $\rho_o = \rho_f \equiv 1000$ kg/m^3 (freshwater); (b) $\rho_o = \rho_{min} \equiv$

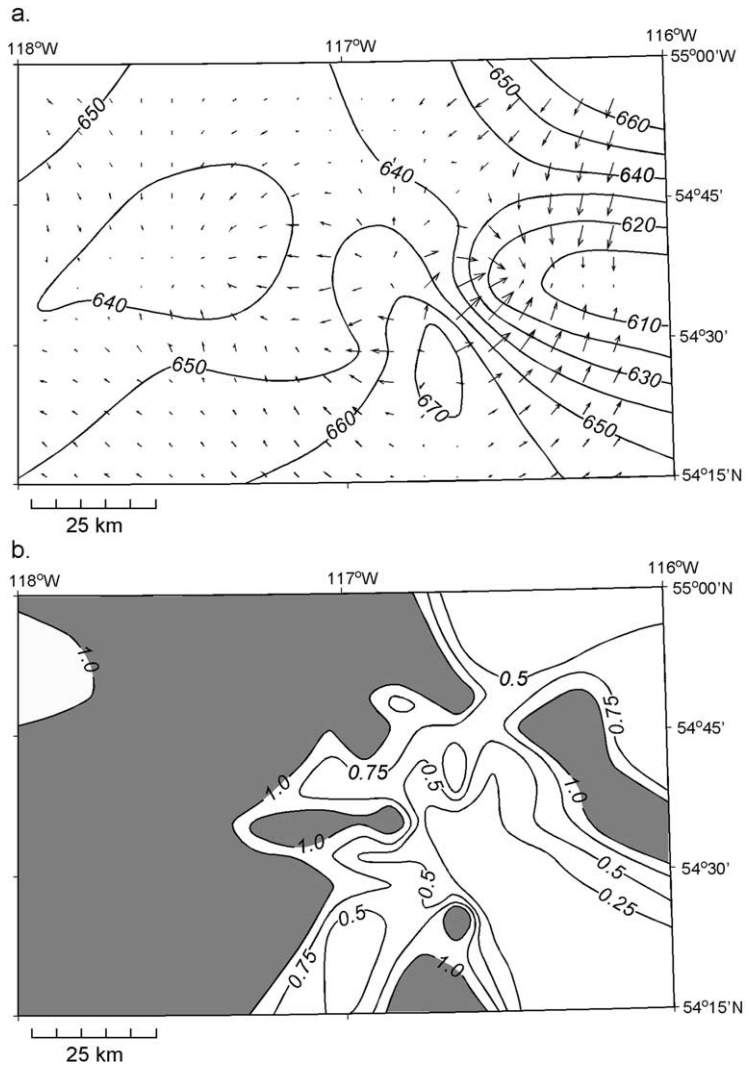

Fig. 12. Flow representation using the minimum density, $\rho_{min} = 1085$ kg/m^3, as reference density: (a) distribution of hydraulic heads, overlain by the flow-driving force field; and (b) distribution of the DFR. Shaded areas represent DFR > 1.

1088 kg/m^3; (c) $\rho_o = \rho_{max} \equiv 1136$ kg/m^3; (d) $\rho_o = \rho_{av} \equiv 1121$ kg/m^3 (density areal-average); and (e) $\rho_o = \rho_{ar} \equiv 1112$ kg/m^3 (arithmetic average of the density variability range). Figs. 11–14 show, for representative reference-density values, the distributions of the corresponding hydraulic heads and DFRs. For representation purposes only, the DFR values are contoured only up to DFR $= 1$, and shaded for DFR > 1. The distribution of the flow-driving force **F**, which indicates the actual flow direction and magnitude, is superimposed over each potentiometric surface. Freshwater hydraulic heads vary from >960 m in the SW to <840 m in the east, and generally would suggest an east-northeasterly flow direction (Fig. 11a). However, the distribution of the flow-driving force **F** broadly indicates flow in the eastern third of the study area towards the 840 m hydraulic head minimum, and westward flow in the western 2/3 of the study area. In places, the flow direction is along, rather than across the freshwater hydraulic head isocontour lines (e.g. in the SW), or even opposite to the direction suggested by ∇H_f (e.g. along the 920 m

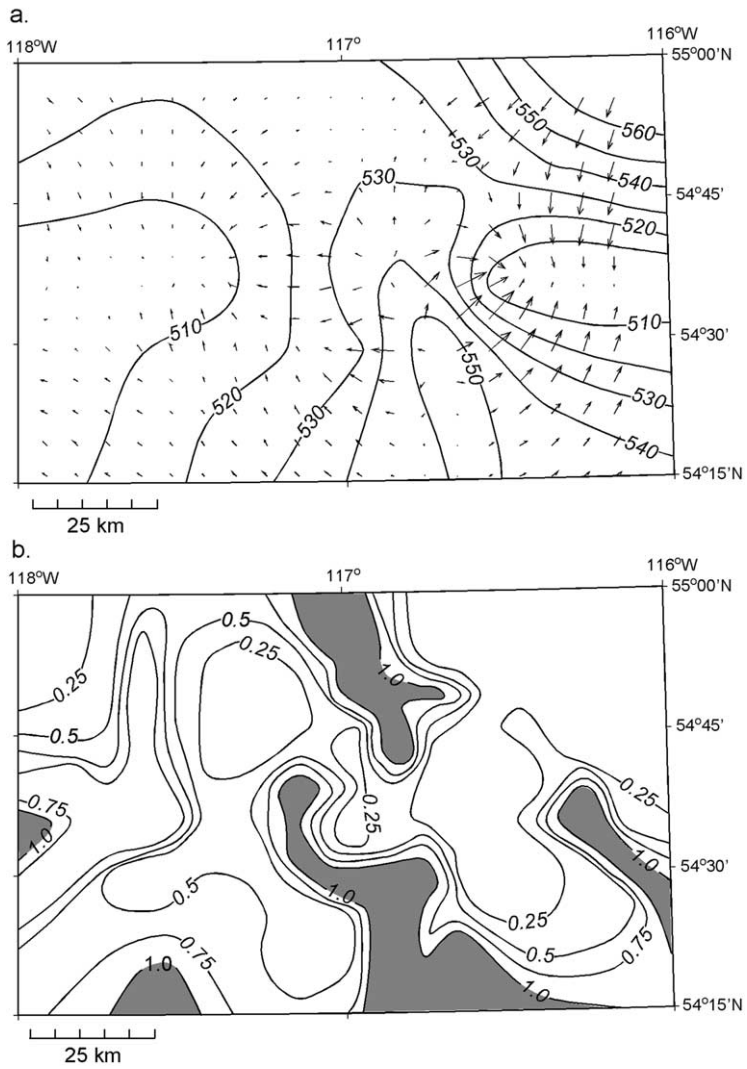

Fig. 13. Flow representation using the maximum density, $\rho_{max} = 1135$ kg/m^3, as reference density: (a) distribution of hydraulic heads, overlain by the flow-driving force field; and (b) distribution of the DFR. Shaded areas represent DFR > 1.

contour line in the north, Fig. 11). The DFR is generally >1 almost everywhere, with an areal average of 4.5, except for a region located in the eastern third of the study area (Fig. 11b). This region corresponds to that part of the aquifer where the potential component $\mathbf{F}_p$ of the flow-driving force $\mathbf{F}$ is the largest, and the errors in direction and magnitude are the smallest (Fig. 11b). In any other part of the aquifer, the errors in direction and/or in magnitude are significant enough to completely distort and misrepresent the flow (Fig. 11b).

Hydraulic heads calculated with $\rho_o = \rho_{min}$ vary in the 610–670 m range (Fig. 12a) and correctly predict the flow direction and strength in the eastern third of the study area. The flow in the western 2/3 is better represented, although errors in direction are still present, particularly in the W–NW. This is consistent with the DFR distribution (Fig. 12b), where DFR < 1 over most of the eastern third of the study area, and >1 over the western 2/3, with an areal average of 2.3, overall lower than in the case for $\rho_o = \rho_f$. The flow radiates from a local hydraulic-head high of 670 m in

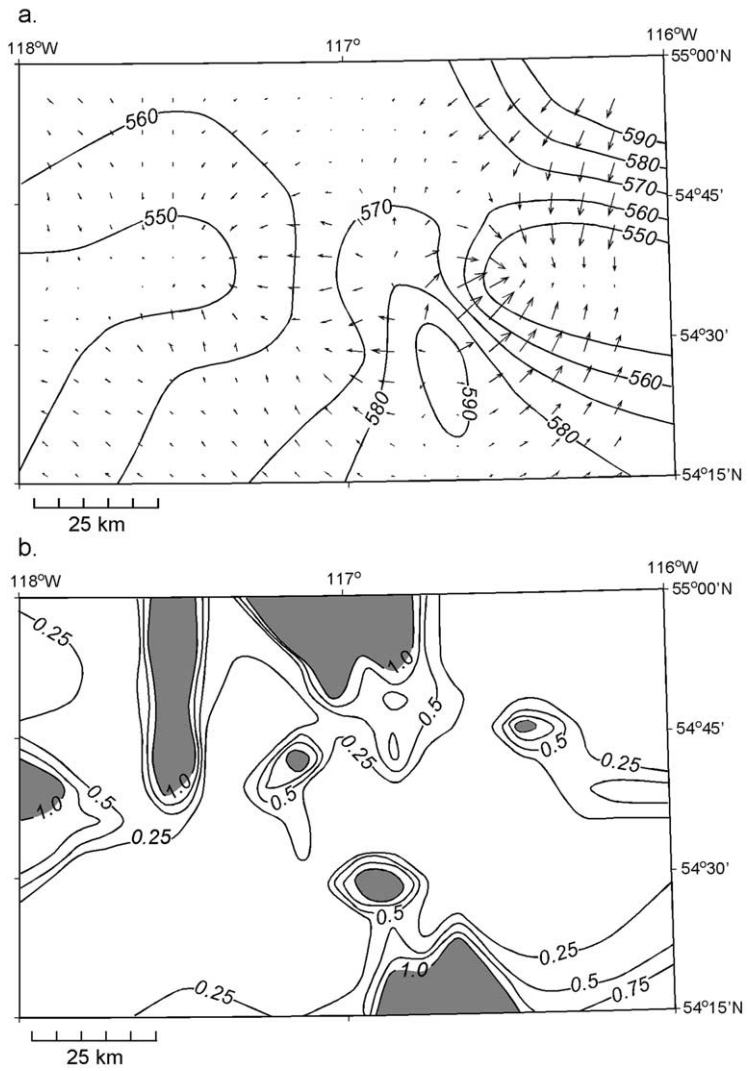

Fig. 14. Flow representation using the areally-weighted average density, $\rho_{av} = 1121$ kg/m^3, as reference density: (a) distribution of hydraulic heads, overlain by the flow-driving force field; and b) distribution of the DFR. Shaded areas represent DFR > 1.

the center-southeast, and converges towards the 610 m low in the east and the <640 m low in the center-west (Fig. 12a). Hydraulic heads calculated with $\rho_o = \rho_{max}$ vary in the 510–560 m range (Fig. 13a) and correctly predict the flow direction and strength over most of the study area. In the center-southwest, hydraulic heads suggest flow from a high hydraulic-head tongue, contrary to the radiating flow pattern indicated by the flow-driving force, while in the west flow is towards a <510 m low, west of the 510 m contour line. The DFR is even lower than in the case of $\rho_o = \rho_{min}$ (Fig. 13b), with an areal average of 1.2. The regions where the flow is still incorrectly depicted by hydraulic-head distributions, particularly in terms of local direction, correspond to the DFR > 1 (Fig. 13). Finally, hydraulic heads calculated with the field density average $\rho_o = \rho_{av}$, which vary in the 550–590 m range, seem to be the best predictor in terms of flow direction and strength (Fig. 14a), correctly showing, beside the strong features, the radiating flow from the hydraulic-head high in the center-southwest, and the flow towards the <550 m low west of the 550 m

contour line. The DFR is the lowest of all cases presented, with an areal average of 0.6 (Fig. 14b). The case of hydraulic heads calculated with the arithmetic average $\rho_o = \rho_{ar}$ (not shown) is not as good as the case of the field density average, $\rho_o = \rho_{av}$, but it is still better than all the others, with an average DFR = 0.9.

The previous example from the Alberta basin, based on actual data, shows rather convincingly that the accuracy in estimating the direction and magnitude of variable-density flow in sloping aquifers on the basis of hydraulic-head distributions depends to the largest degree on the choice of the reference density ρ_o used in calculations. In order to improve the accuracy and minimize errors, the reference density should be within the range of density variations within the aquifer(s) under study. It should not be at either extreme, but at an optimum value that is the areally-weighted average of density. If the areal average is not known, then the next best approximation would be the simple arithmetic average of the observed density values. This result is consistent with Jorgensen et al. (1982) recommendation to use the average density between two observation wells when trying to establish if flow takes place between these two wells, or if hydrostatic conditions prevail. Since the freshwater density is either at the low end of the density-variation spectrum, or outside it, the use of freshwater hydraulic-head distributions in the representation and analysis of such flow systems introduces errors that in many cases may be significant.

5. Conclusions

The representation and analysis of the flow of formation waters in sedimentary basins pose challenges among which the high variability in water density and aquifer geometry appear very early in the process of interpretation, and, as such, are quite important. The variations in water density introduce a buoyancy component to the flow-driving force that is not derived from a potential field, unlike the pressure (potential) component. Thus, the use of hydraulic-head surfaces in the representation and analysis is, at least theoretically, inadequate. Numerical models address this issue by using primary variables, such as pressure, temperature and salinity, in the analysis. However, even when numerical modeling is being used, the distributions of primary variables and other parameters, such as permeability and porosity, are usually not known or very poor, and there is need for at least a preliminary representation, analysis and interpretation of the flow based on observed and/or measured data, to establish boundary and initial conditions and to validate modeling results.

Historically, distributions of freshwater hydraulic heads have been used to represent and analyze the formation water flow in sedimentary basins. However, these distributions provide a correct indication of the strength and direction of the lateral component of the flow-driving force only in the case of horizontal and near-horizontal aquifers, while distributions of environmental hydraulic heads provide the same information regarding the vertical component. Since most aquifers in sedimentary basins are sloping and confined (hence vertically discontinuous), the buoyancy component of the flow-driving force cannot be a priori neglected anymore. Using variable-density hydraulic heads in the analysis contravenes Darcy's law. Thus, the distributions of constant-density hydraulic heads remain the only available tool for representation and analysis of variable-density flow in sloping aquifers, short of calculating the driving force or Darcy velocity over the entire flow domain. Although this is the simplest and quickest means of analysis, one should be fully aware of the errors associated with the use of this tool.

A first error is introduced when approximating the potential and buoyancy components along aquifer slope of the flow-driving force with their projections onto the horizontal plane, for the plan-view flow analysis in the gravity-based Cartesian system. This error can be neither quantified nor its significance evaluated, but it is most probably negligibly small for the small angles of strata inclination usually encountered in undisturbed sedimentary basins. For aquifers dipping at a significant angle, such as in folded strata, this error is probably significant.

A second error is introduced when using only hydraulic heads in the representation and analysis, and neglecting the buoyancy component of the flow-driving force. This error manifests itself in both magnitude and direction of the flow-driving force, and cannot be quantified unless the force itself is calculated, thus defeating the purpose of using this tool in the analysis. However, the significance of

this error can be assessed by performing a DFR analysis at selected critical points. Since the DFR has no threshold, or critical value, hydraulic heads alone can be used only for small DFR values (DFR < 1). Generally, the smaller the DFR is, the smaller are the errors in using only hydraulic heads.

The errors introduced by the use of a constant density in hydraulic head calculations and flow interpretation cannot be avoided for variable-density flow in sloping aquifers, but can be minimized. In most cases the use of freshwater as the reference density actually maximizes these errors. The reference density ρ_o used in calculating hydraulic heads should at least be within the range of density-variation within the aquifer. The optimum value for the reference density that minimizes the error significance (DFR), hence the error in representing, analyzing and interpreting the variable-density flow in a sloping aquifer using hydraulic heads only, is the areally-weighted average of water density observed in that aquifer.

References

Bachu, S., 1995a. Flow of variable-density formation water in deep sloping aquifers: review of methods of representation with case studies. J. Hydrol. 164, 19–38.

Bachu, S., 1995b. Synthesis and model of formation-water flow, Alberta basin, Canada. Bull. Am. Assoc. Petrol. Geol. 79, 1159–1178.

Bachu, S., Burwash, R.A., 1991. Regional-scale analysis of the geothermal regime in the Western Canada sedimentary basin. Geothermics 20 (5/6), 387–407.

Bachu, S., Hitchon, B., 1996. Regional-scale flow of formation waters in the Williston basin. Bull. Am. Assoc. Petrol. Geol. 80, 248–264.

Bear, J., 1972. Dynamics of Fluids in Porous Media. Elsevier, Amsterdam 764pp.

Bethke, C.M., 1985. A numerical model of compaction-driven groundwater flow and heat transfer and its application to the paleohydrology of intracratonic basins. J. Geophys. Res. 90, 6817–6828.

Davies, P.B., 1987. Modeling areal, variable-density, ground-water flow using equivalent freshwater head—analysis of potentially significant errors. Proceedings of the NWWA-IGWMC Conference—Solving Groundwater Problems with Models. 10–12 February 1987, Denver, CO. National Water Well Association, Dublin, OH pp. 888–903.

de Marsily, G., 1986. Quantitative Hydrogeology. Academic Press, San Diego, CA 440pp.

Deming, D., Nunn, J.A., 1991. Numerical simulations of brine migration by topographically driven recharge. J. Geophys. Res. 96 (B2), 2485–2499.

DeWiest, R.J.M., 1965. Geohydrology. Wiley, New York 366pp.

Dorgarten, H-W., Tsang, C-F., 1991. Modelling the density-driven movement of liquid wastes in deep sloping aquifers. Ground Water 29 (5), 655–662.

Frind, E.O., Matanga, G.B., 1985. The dual formulation of flow transport modeling; 1. Review of theory and accuracy aspects. Water Resour. Res. 21 (2), 159–169.

Garven, G., Freeze, R.A., 1984. Theoretical analysis of the role of groundwater flow in the genesis of stratabound ore deposits, 1. Mathematical and numerical model. Am. J. Sci. 284, 1085–1124.

Gupta, N., Bair, E.S., 1997. Variable-density flow in the midcontinent basins and arches region of the United States. Water Resour. Res. 33 (8), 1785–1802.

Hubbert, M.K., 1940. Theory of ground-water motion. J. Geol. 48, 785–944.

Hubbert, M.K., 1953. Entrapment of petroleum under hydrodynamic conditions. Bull. Am. Assoc. Petrol. Geol. 37, 1954–2026.

Hubbert, M.K., 1956. Darcy law and the field equations of the flow of underground fluids. Trans. Am. Inst. Min. Metal. Engng. 207, 222–239.

Jorgensen, D.G., Gogel, T., Signor, D.C., 1982. Determination of flow in aquifers containing variable-density water. Ground Water Monit. Rev. 2 (2), 40–45.

Kuiper, L., 1983. A numerical procedure for the solution of steady state variable density groundwater flow equation. Water Resour. Res. 19 (1), 234–240.

Lahm, T.D., Bair, E.S., VanderKwaak, J., 1998. Role of salinity-derived variable-density flow in the displacement of brine from a shallow, regionally extensive aquifer. Water Resour. Res. 34 (6), 1469–1480.

Lusczynski, N.J., 1961. Head and flow of ground water of variable density. J. Geophys. Res. 66 (12), 4247–4255.

McCain Jr., W.D., 1991. Reservoir-fluid property correlations—state of the art. Soc. Pet. Eng. Reserv. Engng 6, 266–272.

Michael, K., Bachu, S., 2001. Fluids and pressure distributions in the foreland-basin succession in the west-central part of the Alberta basin, Canada: evidence for permeability barriers and hydrocarbon generation and migration. Bull. Am. Assoc. Petrol. Geol. 85, 1231–1252.

Neuzil, C.E., 1986. Groundwater flow in low-permeability environments. Water Resour. Res. 22, 1163–1195.

Oberlander, P.L., 1989. Fluid density and gravitational variations in deep boreholes and their effect on fluid potential. Ground Water 23 (3), 341–350.

Ophori, D.U., 1999. Constraining permeabilities in a large-scale groundwater system through model calibration. J. Hydrol. 224, 1–20.

Senger, R., Fogg, G.E., 1990a. Stream functions and equivalent fresh-water heads for modeling regional flow of variable-density ground water, part 1 of review of theory and verification. Water Resour. Res. 26, 2089–2096.

Senger, R., Fogg, G.E., 1990b. Stream functions and equivalent fresh-water heads for modeling regional flow of variable-density ground water, part 2 of applications and implications for modeling strategy. Water Resour. Res. 26, 2097–2106.